

Electronic Supplementary Information (ESI)

Dual Responsive Photonic Liquid for Independent Modulation of Color Brightness and Hue

Yun Liu,^{a, c} Qingsong Fan,^c Guanghao Zhu,^b Gongpu Shi,^a Huiru Ma,^{*b} Wei Li,^a Tianlong Wu,^a Jitao Chen,^a Yadong Yin^{*c} and Jianguo Guan^{*a}

^a State Key Laboratory of Advanced Technology for Materials Synthesis and Processing, International School of Materials Science and Engineering, Wuhan University of Technology, Wuhan 430070, China. *E-mail: guanjg@whut.edu.cn.

^b Department of Chemistry, School of Chemistry, Chemical Engineering and Life Science, Wuhan University of Technology, Wuhan 430070, China. *E-mail: mahr@whut.edu.cn.

^c Department of Chemistry, University of California, Riverside, CA 92521, USA. *E-mail: yadong.yin@ucr.edu.

Chemical reagents: Ferric chloride hexahydrate ($\text{FeCl}_3 \cdot 6\text{H}_2\text{O}$, AR), sodium acetate (NaAc, AR), Poly (vinyl pyrrolidone) (PVP, K-30, GR), ethylene glycol (EG, AR), and ethanol (AR) were purchased from Sinopharm Chemical Reagent Co. Ltd. N, N'-methylene-bis-acrylamide (BIS, 99%), 2-hydroxy-2-methylpropiophenone (HMPP, 97%) and tannic acid (TA, AR) were purchased from Aladdin Reagent (Shanghai) Co. Ltd. N-isopropyl acrylamide (NIPAM, 98%) and poly(acrylic acid) aqueous solution (PAA, MW=800–1000, 30%) were obtained from Shanghai Macklin Biochemical Co. Ltd. and Tianjin Kermel Chemical Reagents Co. Ltd., respectively. All chemicals were used as received.

Preparation of the Fe_3O_4 @PVP CNCs: The building blocks of monodisperse Fe_3O_4 @PVP CNCs (Fig. S1) were prepared by a modified solvothermal method.¹ Typically, 0.13 mmol PVP and 0.053 mmol TA were dissolved into 30 mL EG. The obtained solution was heated at 130 °C with vigorous stirring for 20 min to obtain a transparent solution and subsequently cooled down to 70 °C. Then, 2.0 mmol $\text{FeCl}_3 \cdot 6\text{H}_2\text{O}$ were added into the solution and stirred for 40 min. Afterward, the solution was cooled down to 20 °C and 34 mmol NaAc were added into the homogeneous mixture. After 40 min of vigorous stirring, the resultant solution was transferred into a 100 mL Teflon-lined stainless-steel autoclave and kept at 200 °C for 12 h. Finally, the black products were collected by a magnet and rinsed with ethanol for three times and stored in 20 mL ethanol. The Fe_3O_4 @PVP CNCs EG dispersion were obtained by centrifuging the Fe_3O_4 @PVP CNCs ethanol dispersion and then dispersing the Fe_3O_4 @PVP CNCs in EG.

Preparation of the Fe_3O_4 @PVP@PNIPAM flexible PNCs: The Fe_3O_4 @PVP@PNIPAM flexible PNCs were obtained by a hydrogen bond-guided template polymerization method.² Typically, a precursor solution was firstly prepared by dissolving 0.3 g NIPAM, 20.4 mg BIS and 30.0 mg HMPP in 1.0 mL Fe_3O_4 @PVP CNCs EG dispersion with a particle concentration of 2.3 $\text{mg} \cdot \text{mL}^{-1}$. Then, 200 μL of the solution was mixed with 2.0 mL 0.83 $\text{mg} \cdot \text{mL}^{-1}$ PAA aqueous solution in a glass beaker by ultrasonic treatment for 5

s. Afterward, the beaker was placed above the center of a 10×10×2 cm NdFeB square magnet with a distance of 1.5 cm (725 Gs) for 30 s. Finally, a 365 nm UV lamp with a vertical distance of 5 cm from the beaker was turned on and kept for 120 s. The well dispersed brown flocculent products could be observed after the photo-polymerization reaction and they were collected by centrifuging and washing with ethanol for two times. The final products were dispersed in water or ethanol for further use. Flexible Fe₃O₄@PVP@PNIPAM PNCs with different chain lengths, cross-linking degrees, and interparticle distances could be obtained by varying the concentration of Fe₃O₄@PVP CNCs (*c*), the molar ratio of BIS and NIPAM (δ) and the strength of *H*.

Characterization: The morphology, microstructure, and composition of the samples were characterized by field-emission scanning electron microscope (FE-SEM, Hitachi S-4800, 10 kV), high-resolution transmission electron microscope (HRTEM, JEOL JEM-2100F, 200 kV), and Fourier-transforming infrared (FT-IR, Nicolet, 60SXB, 4000–400 cm⁻¹, room temperature) spectrometer. Thermogravimetric /differential scanning calorimetric (TG-DSC) analysis was carried out on a NETZSCH-STA449F3 thermal analyzer from room temperature to 1000 °C under air atmosphere with a heating rate of 10 °C·min⁻¹. The optical microscopy videos and images were recorded by an optical microscope (Leica DMI 3000 M). The bright-field images and videos were obtained from an ethanol suspension of the flexible PNCs. The dark-field images for the typical samples were obtained from their aqueous suspension. The dark-field images for the flexible PNCs obtained under *H* = 200 and 1900 Gs and δ = 1% and 10% were obtained from their ethanol suspensions. The magnetic field during the optical observation is supplied by a 5×5×2 cm NdFeB circle magnet.

Measurement of magnetic and optical properties: The magnetic hysteresis loop of the typical sample was measured using a physical property measurement system (PPMS, Model PPMS-9, Quantum Design) with applied magnetic fields between -20 and 20 kOe at 300 K. The reflection spectra were recorded using a fiber optic spectrometer (Ocean Optics, USB2000+). The uniform external *H* was supplied by a Helmholtz loop and the field strength was controlled by a DC regulated power supply (WYJ-5010D, China). The reflection spectra of the typical flexible PNCs under different *T* and *H* and the flexible PNCs with δ = 2% and 10% under different *T* were collected from their aqueous suspension. The magnetic field strength dependent reflection spectra of other samples were collected from their ethanol suspensions.

Numerical simulation: A quasi-3D simulation experiment was conducted to qualitatively study the relationship between the strength of applied *H* and the conformations of the Fe₃O₄@PVP@PNIPAM flexible PNCs by MATLAB. The detailed description about the calculation model and the corresponding simulation was illustrated in the following text.

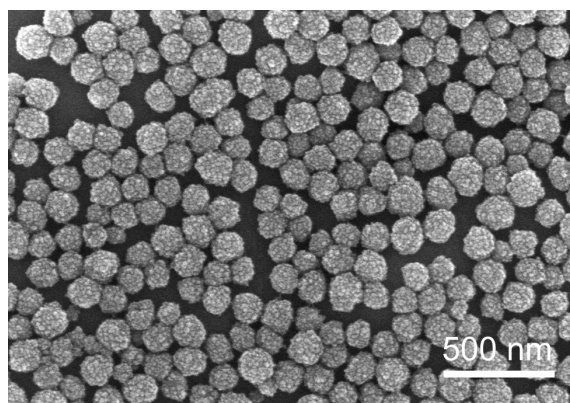


Fig. S1 SEM image of the $\text{Fe}_3\text{O}_4@\text{PVP}$ CNCs.

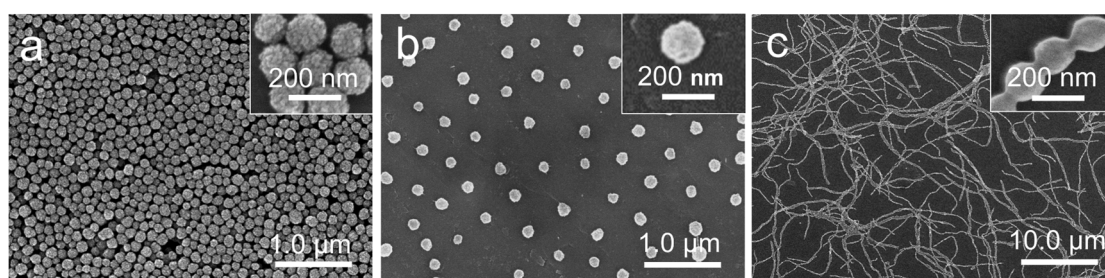


Fig. S2 SEM images of the products obtained under different PAA concentration. (a) 0; (b) $0.31 \text{ mg}\cdot\text{mL}^{-1}$; (c) $1.67 \text{ mg}\cdot\text{mL}^{-1}$.

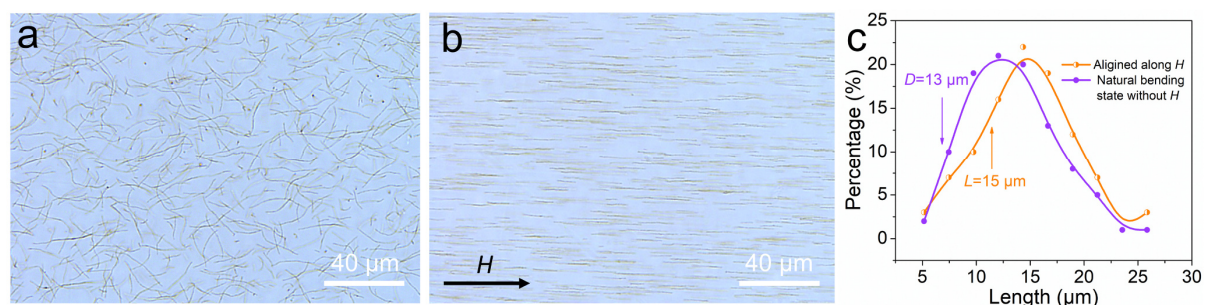


Fig. S3 (a, b) Bright-field optical microscopy images of the typical $\text{Fe}_3\text{O}_4@\text{PVP}@\text{PNIPAM}$ flexible PNCs under different orientation state. (a) Natural bending state without H ; (b) Aligned state under H . (c) The corresponding distribution of the end-to-end distance (D) of the bent nanochains and the average chain length (L) of the aligned nanochains, which were calculated by measuring 100 dispersed chains in (a) and (b).

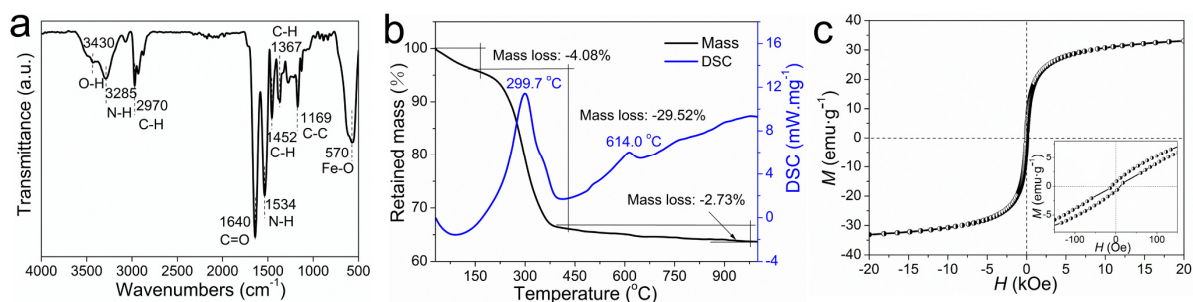


Fig. S4 The composition and magnetic property of the typical $\text{Fe}_3\text{O}_4@\text{PVP}@\text{PNIPAM}$ flexible PNCs. (a) FT-IR spectrum, (b) TG and DSC curves and (c) magnetic hysteresis loop. The low right inset in (c) shows the expanded region around the origin.

The presence of PVP, PAA and PNIPAM and the formation of hydrogen bonds between them were confirmed by the FT-IR spectrum. As shown in Fig. S4a, the peak at 3430 cm^{-1} corresponds to the stretching vibration of O–H in PAA, and the peaks at 3285 and 1534 cm^{-1} correspond to the stretching and flexural vibrations of N–H in PNIPAM. Furthermore, the isopropyl groups ($-\text{CH}(\text{CH}_3)_2$) show a peak at 2970 cm^{-1} , and the asymmetric and symmetric stretching vibrations of methyl groups ($-\text{CH}_3$) result in the peaks at 1452 and 1367 cm^{-1} .^{3,4} The typical peak of carbonyl group ($-\text{C}=\text{O}$) blue shifts from 1652 cm^{-1} to 1640 cm^{-1} , which suggests that PAA generates hydrogen bonds with both PVP and PNIPAM. The characteristic peak of Fe–O in Fe_3O_4 presents at 570 cm^{-1} . The mass percentage of polymers can be calculated from the TG data. As shown in Fig. S4b, the TG curve exhibits a three-step weight loss. The mass loss of 4.08% before $150\text{ }^\circ\text{C}$ is caused by the removal of adsorbed water or surface hydroxyls.⁵ The main weight loss of 29.52% and exothermic peaks at $299.7\text{ }^\circ\text{C}$ occurring in the range of $150\text{--}400\text{ }^\circ\text{C}$ is due to the decomposition of organic polymers. The last weight loss between $400\text{--}1000\text{ }^\circ\text{C}$ is the comprehensive effect of the decomposition of carbon residues⁶ and the transformation of Fe_3O_4 to $\alpha\text{-Fe}_2\text{O}_3$. The exothermic peak at $614.0\text{ }^\circ\text{C}$ is attributed to the conversion of Fe_3O_4 to $\alpha\text{-Fe}_2\text{O}_3$ in air atmosphere.⁷ During the heating process, organic polymers were completely burnt to CO_2 and Fe_3O_4 was finally transformed to Fe_2O_3 . Thus, the remaining product was Fe_2O_3 . the mass percentage of polymers is calculated as 34.37% by using the equation of

$$\text{wt}\%_{\text{polymers}} = 1 - \text{wt}\%_{\text{H}_2\text{O}} - \text{wt}\%_{\text{remains}} \frac{M_{\text{Fe}_3\text{O}_4}}{1.5M_{\text{Fe}_2\text{O}_3}} \quad (1)$$

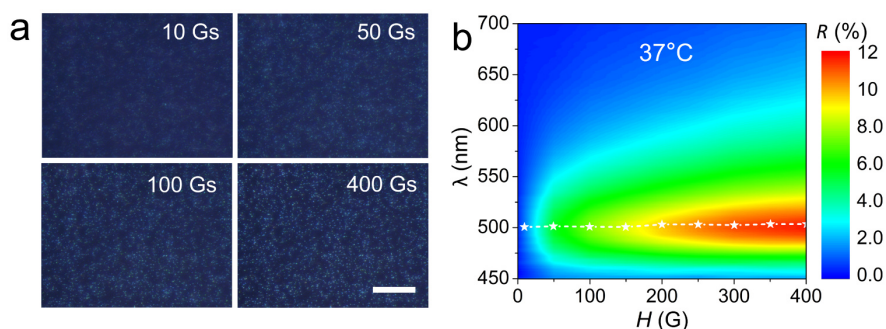


Fig. S5 (a) Dark-field optical microscopy images and (b) 2D contour map of the reflection spectra of the typical $\text{Fe}_3\text{O}_4@\text{PVP}@\text{PNIPAM}$ flexible PNCs obtained under different H at 37 °C. The scale bar in (a) is 100 μm .

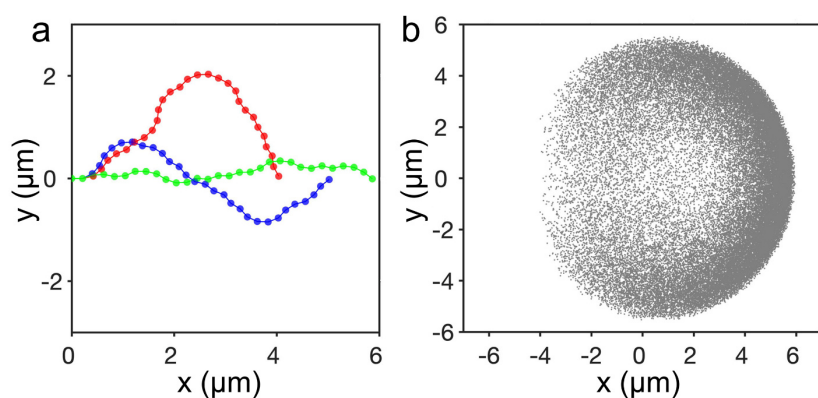


Fig. S6 (a) Three typical flexible PNCs with different end-to-end distance; (b) Plots of the tail-end locations of the 50,000 chains without H .

A quasi-3D simulation experiment was conducted by MATLAB to qualitatively illustrate the relationship between the strength of applied H and the conformations of the flexible PNCs. In the simulation, the probability of different conformations under different H was calculated based on their total energy. To simplify the calculation, flexible chain composed by 30 nanospheres with the diameter of 140 nm and equal interparticle distance of 212 nm was used as the model chain. The values of nanosphere diameter and the interparticle distance were set based on the typical $\text{Fe}_3\text{O}_4@\text{PVP}@\text{PNIPAM}$ flexible PNCs at 30 °C. The positions of the first two spheres are fixed around the origin, and positions of the rest of 28 spheres are generated randomly with the restriction of bond angles (θ). Three typical flexible chains with different bending states and end-to-end distances are given in Fig. S6a. For the probability calculation, 50,000 flexible chains with different conformations are considered and the locations of their last spheres are plotted in Fig. S6b.

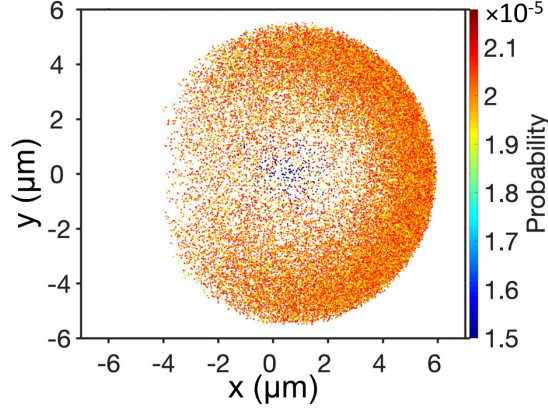


Fig. S7 The conformation probabilities of the 50,000 chains without H .

Three interactions are considered during the energy calculation, namely Weeks–Chandler–Andersen (WCA) interaction, bonded interaction and magnetic dipole-dipole interaction, which are illustrated as follows:

WCA interaction: To prevent the overlapping of spheres in the chains, a repulsive WCA potential is used:

$$U_{ij}^{WCA} = \begin{cases} 4\epsilon \left(\left(\frac{\sigma}{d_{ij}} \right)^{12} - \left(\frac{\sigma}{d_{ij}} \right)^6 \right) + \epsilon, & d_{ij} \leq 2\frac{1}{6}\sigma \\ 0, & d_{ij} > 2\frac{1}{6}\sigma \end{cases} \quad (2)$$

where $\epsilon = k_B T$, $k_B = 1.38 \times 10^{-23} \text{ J} \cdot \text{K}^{-1}$, $T = 300 \text{ K}$; $\sigma = 2^{-\frac{1}{6}} d_0$, $d_0 = 212 \text{ nm}$; and d_{ij} is the center-center distance between the two particles.⁸

Bonded interaction: A bead-spring model, which is often used when simulating the behavior of single polymer chain, is employed to represent the interaction between neighboring particles due to the inter-connecting polymer chains. For a quasi-3D model, the bonded interaction includes stretching U_i^r and U_i^θ bending parts:

$$U_i^r = \frac{1}{2} K_r (d_{i,i+1} - d_0)^2 \quad (3)$$

$$U_i^\theta = \frac{1}{2} K_\theta (\theta_i - \theta_0)^2 \quad (4)$$

where d_0 is the equilibrium bond distance (212 nm), K_r is the linear stiffness of the bond ($k_B T$); K_θ is the bending rigidity ($k_B T$), θ_0 is the equilibrium bond angle.⁹ In fact, θ is a free parameter, we can set it as any value. When it was set as 20° , the generated conformations of the soft nanochains were closest to the experimental observations. We chose 20° as the equilibrium bond angle (θ_0).

Magnetic dipole-dipole interaction: In the presence of an applied magnetic field, the nanoparticles are magnetized. The potential energy for two dipoles is given by:

$$U_{ij}^{dd} = -\frac{\mu_0}{4\pi} \left(3 \frac{(\mathbf{m}_{i,\text{eff}} \cdot \mathbf{d}_{ij})(\mathbf{m}_{j,\text{eff}} \cdot \mathbf{d}_{ij})}{d_{ij}^5} - \frac{\mathbf{m}_{i,\text{eff}} \cdot \mathbf{m}_{j,\text{eff}}}{d_{ij}^3} \right) \quad (5)$$

Where $\mu_0 = 4\pi \times 10^{-7} \text{ H}\cdot\text{m}^{-1}$, $\mathbf{m}_{i,\text{eff}}$ and $\mathbf{m}_{j,\text{eff}}$ are the moments of i 'th and j 'th particle, and \mathbf{d}_{ij} is the displacement vector between them. The magnetic dipole moment of particles in a chain is supposed to have the same dipole moment, which can be calculated by¹⁰

$$\mathbf{m}_{i,\text{eff}} = \mathbf{m}_{j,\text{eff}} = \frac{4}{3} \pi r_0^3 \mu_0 \chi \mathbf{H} \quad (5)$$

The effective χ of $7.0 \times 10^{-4} \text{ kg}\cdot\text{m}^{-3}$ is obtained from the hysteresis loop of the typical sample (corrected with the polymer mass percentage from TGA analysis).

Based on the above analysis, the total energy of each chain can be expressed as:

$$U_{\text{chain}} = \sum_{\substack{i=1 \\ i \neq j}}^n (U_{ij}^{WCA} + U_{ij}^{dd}) + \sum_{i=1}^n (U_i^r + U_i^\theta) \quad (6)$$

After calculating the total energy of each configuration, the probability for the conformation i (P_i) is evaluated by partition function:

$$P_i = \frac{e^{-\frac{U_i}{k_B T}}}{\sum_{j=1}^N e^{-\frac{U_j}{k_B T}}} \quad (7)$$

Where N is the total number of conformations, in this case, $N=50,000$.

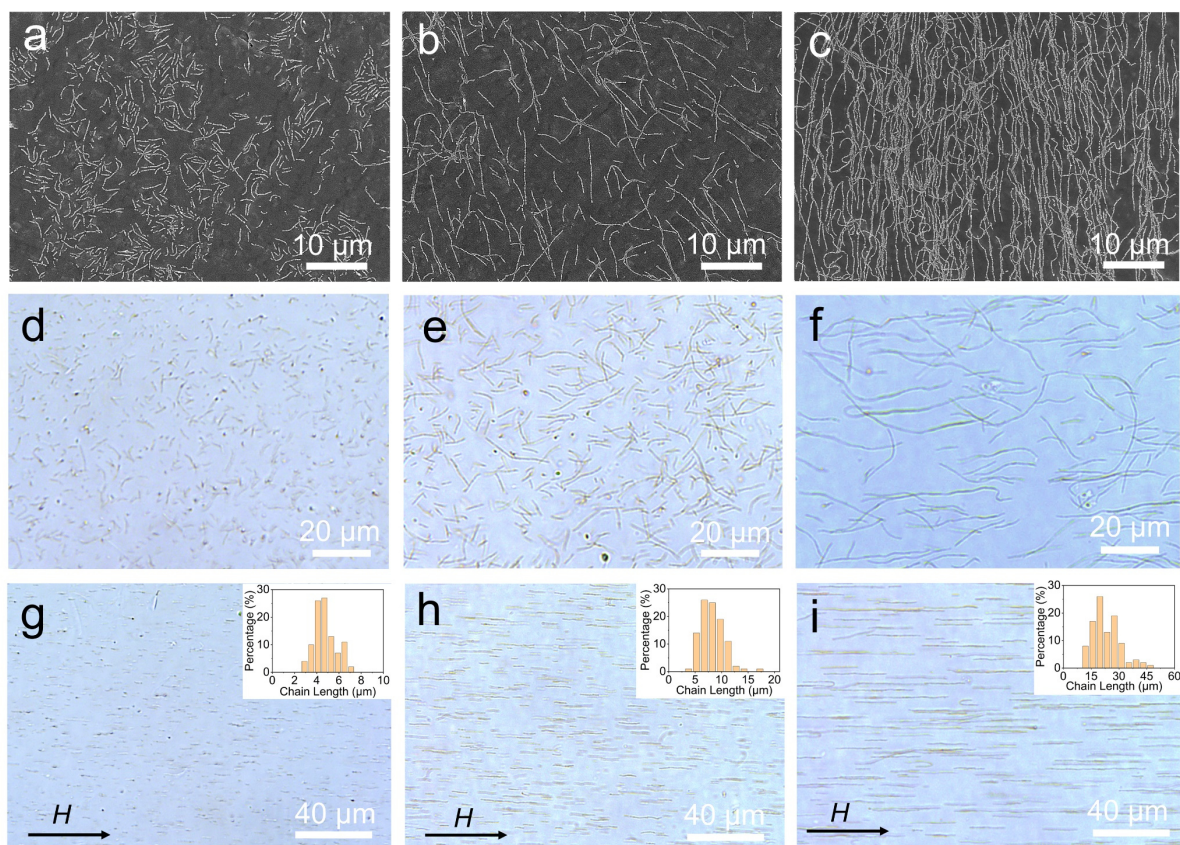


Fig. S8 (a-c) SEM images and (d-i) Bright-field optical microscopy images of $\text{Fe}_3\text{O}_4@\text{PVP}@\text{PNIPAM}$ flexible PNCs with different L obtained by tuning the $\text{Fe}_3\text{O}_4@\text{PVP}$ particle concentration (c) and the strength of H during the preparation process of the flexible PNCs. The insets in (g-i) are the histograms showing the corresponding chain length distribution. (a, d, g) $c = 0.38 \text{ mg}\cdot\text{mL}^{-1}$, $H = 725 \text{ Gs}$, $L = 5 \mu\text{m}$; (b, e, h) $c = 0.76 \text{ mg}\cdot\text{mL}^{-1}$, $H = 725 \text{ Gs}$, $L = 8 \mu\text{m}$; (c, f, i) $c = 2.3 \text{ mg}\cdot\text{mL}^{-1}$, $H = 1900 \text{ Gs}$, $L = 23 \mu\text{m}$.

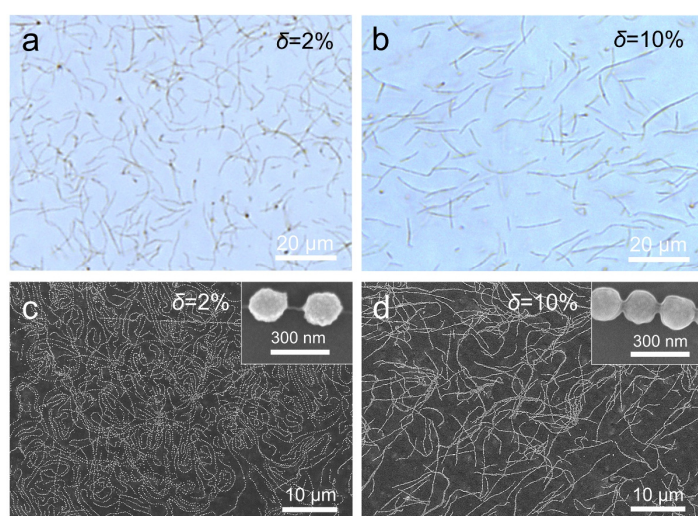


Fig. S9 (a, b) Bright-field optical microscopy images and (c, d) SEM images of the flexible PNCs with different δ .

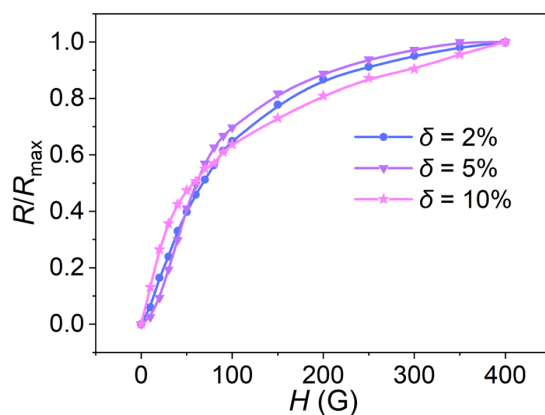


Fig. S10 Plots showing the relationship between H and the relative reflectance (R/R_{\max}) of the PNCs with different δ .

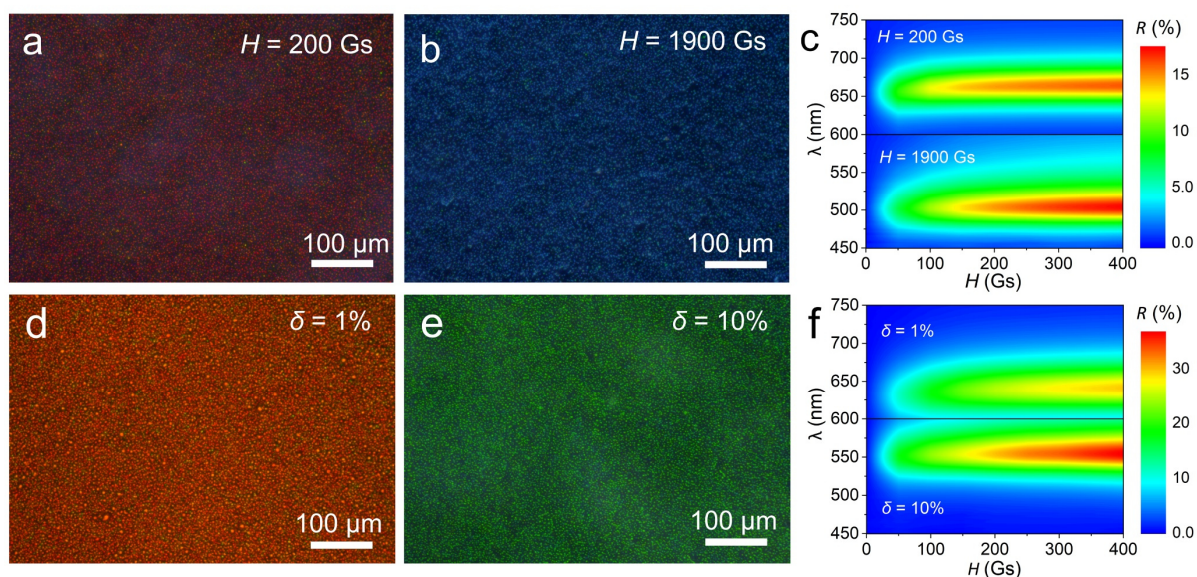


Fig. S11 Dark-field optical microscopy images (a, b, d, e) and the magnetic field strength dependent optical properties (c, f) of the $\text{Fe}_3\text{O}_4@\text{PVP}@\text{PNIPAM}$ flexible PNCs obtained with different H and δ .

Movie S1 Dark field optical video of the typical flexible $\text{Fe}_3\text{O}_4@\text{PVP}@\text{PNIPAM}$ PNCs in response to different H . H first increased from 0 to 400 Gs and then decreased from 400 to 0 Gs.

Movie S2 Dark-field optical video of the typical flexible $\text{Fe}_3\text{O}_4@\text{PVP}@\text{PNIPAM}$ PNCs in response to the stimuli of ice water with T about 4 °C.

Movie S3 Dark-field optical video of the typical flexible $\text{Fe}_3\text{O}_4@\text{PVP}@\text{PNIPAM}$ PNCs in response to the stimuli of warm water with T about 40 °C.

Movie S4 Bright-field optical video of the typical flexible $\text{Fe}_3\text{O}_4@\text{PVP}@\text{PNIPAM}$ PNCs in response to weak magnetic field. H first increased from 0 to 50 Gs and then kept at 50 Gs.

Movie S5 Bright-field optical video of the typical flexible $\text{Fe}_3\text{O}_4@\text{PVP}@\text{PNIPAM}$ PNCs in response to strong magnetic field. H rapidly increased from 0 to 400 Gs and then kept at 400 Gs.

Movie S6 Bright field optical video of the typical flexible Fe₃O₄@PVP@PNIPAM PNCs in response to different strength of *H*. *H* first increased from 0 to 400 Gs and then decreased from 400 to 0 Gs.

Movie S7 Dark-field optical video showing the temperature responsive properties of the Fe₃O₄@PVP@PNIPAM flexible PNCs with $\delta = 2\%$. The temperature stimulation was applied by dropping a drop of warm water with $T=40\text{ }^{\circ}\text{C}$ or ice water with $T=4\text{ }^{\circ}\text{C}$ on the cover glass. The room temperature was $30\text{ }^{\circ}\text{C}$ and the speed of the video was speeded by 8 folds.

Reference

- 1 J. Guan, W. Luo, H. Ma and F. Mou, *China Pat.*, CN103342393B, 2015.
- 2 W. Luo, Q. Cui, K. Fang, K. Chen, H. Ma, J. Guan, *Nano Lett.*, 2020, **20**, 803–811.
- 3 J. Gu, F. Xia, Y. Wu, X. Qu, Z. Yang, L. Jiang, *J. Control. Release*, 2007, **117**, 396–402.
- 4 Q. Zhang, Y. Tang, L. Zha, J. Ma and B. Liang, *Eur. Polym. J.*, 2008, **44**, 1358–1367.
- 5 Y. Liu, Y. Li, K. Jiang, G. Tong, T. Lv and W. Wu, *J. Mater. Chem. C*, 2006, **4**, 7316–7323.
- 6 T. Zhu, J. Chen, X. Lou, *J. Phys. Chem. C*, 2011, **115**, 9814–9820.
- 7 Y. Liu, Y. Fu, L. Liu, W. Li, J. Guan and G. Tong, *ACS Appl. Mater. Interfaces*, 2018, **10**, 16511–16520.
- 8 J. Wei, F. Song, J. Dobnikar, *Langmuir*, 2016, **32**, 9321–9328.
- 9 D. C. Rapaport, *The Art of Molecular Dynamics Simulation*, Cambridge University Press, Cambridge, 2004.
- 10 X. Xue, E. P. Furlania, *Phys. Chem. Chem. Phys.* 2014, **16**, 13306–13317.